



## 20           **Abstract**

21           Virtual libraries for ligand discovery have recently increased 10,000-fold, and this is  
22           thought to have improved hit rates and potencies from library docking. This idea has not, however,  
23           been experimentally tested in direct comparisons of larger-vs-smaller libraries. Meanwhile,  
24           though libraries have exploded, the scale of experimental testing has little changed, with often  
25           only dozens of high-ranked molecules investigated, making interpretation of hit rates and affinities  
26           uncertain. Accordingly, we docked a 1.7 billion molecule virtual library against the model enzyme  
27           AmpC  $\beta$ -lactamase, testing 1,521 new molecules and comparing the results to the same screen  
28           with a library of 99 million molecules, where only 44 molecules were tested. Encouragingly, the  
29           larger screen outperformed the smaller one: hit rates improved by two-fold, more new scaffolds  
30           were discovered, and potency improved. Overall, 50-fold more inhibitors were found, supporting  
31           the idea that there are many more compounds to be discovered than are being tested. With so  
32           many compounds evaluated, we could ask how the results vary with number tested, sampling  
33           smaller sets at random from the 1521. Hit rates and affinities were highly variable when we only  
34           sampled dozens of molecules, and it was only when we included several hundred molecules that  
35           results converged. As docking scores improved, so too did the likelihood of a molecule binding;  
36           hit rates improved steadily with docking score, as did affinities. This also appeared true on re-  
37           analysis of large-scale results against the  $\sigma 2$  and dopamine D4 receptors. It may be that as the  
38           scale of both the virtual libraries and their testing grows, not only are better ligands found but so  
39           too does our ability to rank them.

40

41

42

## 43            **Introduction**

44            With the advent of ultra-large, make-on-demand (“tangible”) libraries, available chemical  
45 space has increased from about 3.5 million to over 38 billion ([https://enamine.net/compound-](https://enamine.net/compound-collections/real-compounds)  
46 [collections/real-compounds](https://enamine.net/compound-collections/real-compounds)). While the size of the new libraries can seem daunting, recent  
47 studies suggest that structure-based docking prioritizes potent ligands from within it, with affinities  
48 often in the mid-nanomolar and sometimes high picomolar range<sup>1-11</sup>. Docking the new libraries  
49 seems to improve hit rates, affinities, and chemotype novelty versus smaller libraries<sup>12,13</sup>,  
50 suggesting that bigger libraries are better for virtual screening. This is supported by simulations  
51 that show that as libraries grow, the best molecules fit ever better to protein binding sites<sup>14</sup>. Exactly  
52 how large libraries affect these key outcomes versus smaller libraries remains to be tested  
53 experimentally in side-by-side studies.

54            Further clouding the issue is the scale of experimental testing of molecules prioritized from  
55 virtual screens. Irrespective of whether million-scale or billion-scale libraries are virtually screened,  
56 rarely are more than several dozen molecules synthesized and tested experimentally<sup>3,6-8</sup>. While  
57 these are high-ranking, they are picked from among a much larger pool of similarly ranked  
58 molecules. From the hit rates of these screens (number active/number-tested), it has been  
59 inferred that there are likely hundreds-of-thousands or even millions of potential ligands in the  
60 libraries that remain untested, but this has not been probed experimentally<sup>1</sup>. As important, the few  
61 molecules tested make the results subject to the statistics of small numbers. Said another way, it  
62 is not clear that we can have full confidence in hit rates, affinity ranges, and the likelihood of  
63 discovering new chemotypes—all key docking outcomes—when testing only a few dozen  
64 compounds.

65            Here we begin to investigate these questions quantitatively. **First**, to explore the impact  
66 of library size on docking outcome, we screened over 1.7 billion molecules for inhibitors of the

67 model enzyme AmpC  $\beta$ -lactamase<sup>1,15-20</sup> and compared the results to a previous screen on the  
68 same enzyme using essentially the same method where only 99 million molecules were docked<sup>1</sup>.  
69 These smaller and larger screens were compared by hit rates, inhibitor affinities, and the number  
70 of novel chemotypes discovered. **Second**, we synthesized and tested 1,521 compounds for  
71 AmpC inhibition, rather than the 44 originally tested in the smaller library campaign<sup>1</sup>, and asked  
72 if the number of inhibitors found scaled with number of top-ranking molecules investigated,  
73 something that has until now simply been an implication of large library docking. **Third**, with these  
74 observations in hand, we examined the sensitivity of docking hit rates and hit affinities to the scale  
75 of experimental testing by sub-sampling smaller sets from the larger one; this has implications for  
76 how we should understand docking hit rates and affinities, and how we should scale these  
77 experiments in the future.

78 **Fourth**, we investigate how hit rate is predicted by docking score, and whether we might  
79 expect better molecules to be found as libraries continue to expand into the tens of billions of  
80 molecules and beyond<sup>5,21</sup>. **Finally**, the scale of the experimental testing here allows us to  
81 investigate potential correlations between docking rank and affinity category (high, mediocre,  
82 poor). We will argue that the answers emerging from this large-scale study support further  
83 expansion of docking libraries into the trillions of compounds range, and, perhaps surprisingly, a  
84 re-investment in docking scoring functions to optimize what is now a loose correlation between  
85 docking rank and affinity category.

86

## 87 **Results**

88 **Selection, synthesis, and testing of 1521 docking hits for AmpC.** With a quantitative  
89 spectrophotometric assay, ability to determine inhibitor-protein crystal structures, and status as a  
90 primary antibiotic resistance mechanism, AmpC  $\beta$ -lactamase has lent itself to multiple structure-

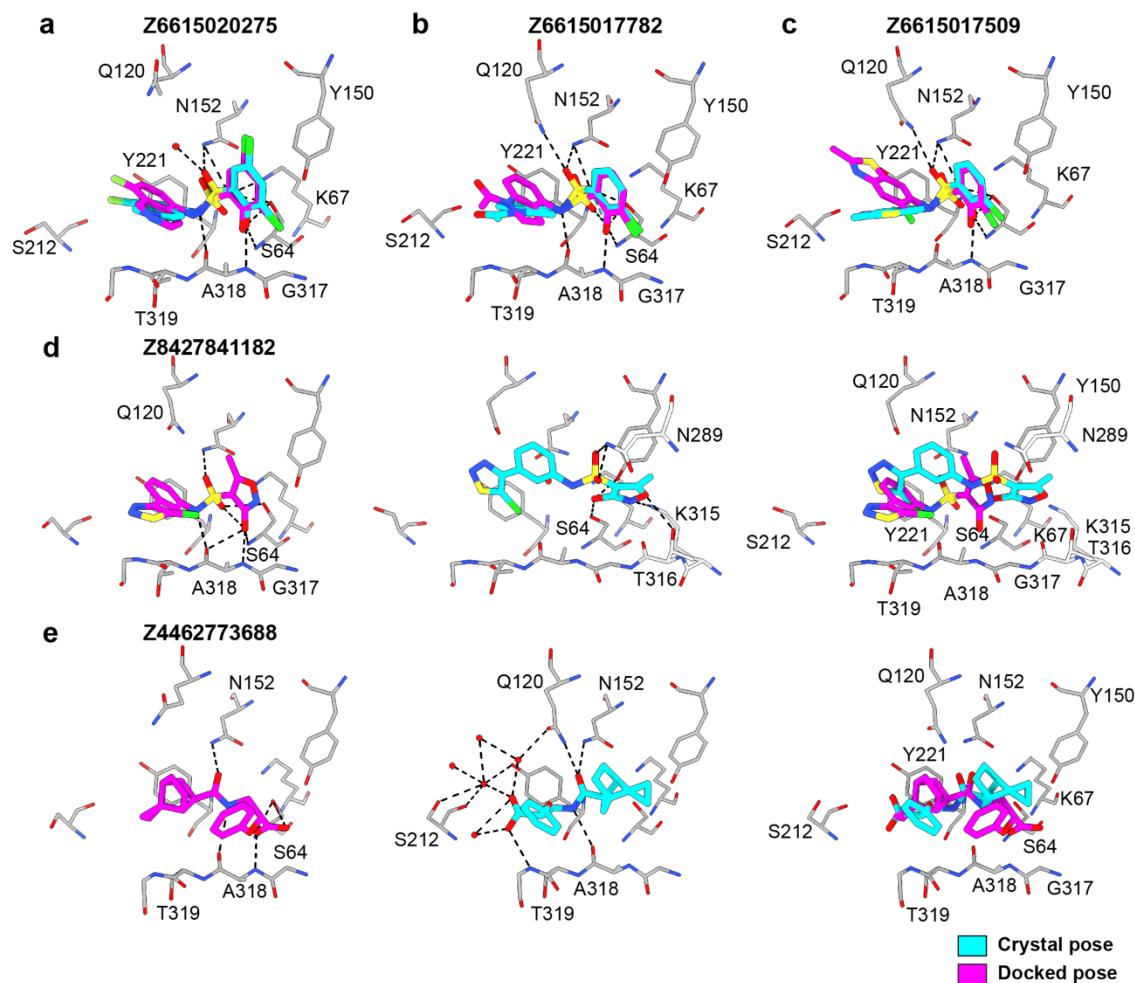
91 based and high-throughput screening campaigns for inhibitor discovery<sup>15-20</sup>, including with ultra-  
92 large libraries<sup>1</sup>, making it a good system to test the impact of library size on virtual screening. In  
93 a previous docking screen of 99 million molecules against the enzyme, 44 high-ranking molecules,  
94 topologically unrelated to previously known scaffolds, were prioritized for synthesis and testing.  
95 This revealed five new inhibitors with affinities ranging from 1.3  $\mu\text{M}$  to 400  $\mu\text{M}$ , a hit rate of 11%  
96 using this range of activity<sup>1</sup>. Using essentially the same docking method, here we screened a 1.7  
97 billion molecule library against the same AmpC active site. Molecules from across the docking  
98 scoring range, 838,672,414 in total ranking from -117.35 kcal/mol (best scores) to -28 kcal/mol  
99 (worst scores), were considered as candidates for experimental testing. These were organized  
100 into bins of resolution ranging from 2 to 4 kcal/mol among the lower (better) scores to 8 kcal/mol  
101 among the higher (worse) scores. Up to 25,000 molecules were selected per bin, by rank order  
102 (for the lower and better energy bins, this amounted to all the molecules in the bin). Molecules  
103 topologically similar to known inhibitors, with ECFP4-based  $T_c > 0.5$ , were excluded, as were  
104 those with more than one unsatisfied hydrogen bond donor and more than six hydrogen bond  
105 acceptors—such molecules exploit known gaps in the DOCK3.8 scoring function<sup>22</sup>. The remaining  
106 193,878 molecules were clustered by  $T_c = 0.32$  based on the interaction fingerprinting<sup>23</sup>, resulting  
107 in 80,767 cluster heads. In previous simulations<sup>14</sup> and experiments<sup>4</sup>, we had found molecules with  
108 artifactually favorable score concentrated among the top-ranking docked molecules. Here too, we  
109 observed molecules that achieved scores much higher than one would expect from the overall  
110 distribution; this problem became more acute as the library grew (**Extended Data Fig. 1**). We  
111 chose to ignore these molecules for experimental testing. The origins of these molecules, and  
112 their experimental confirmation as docking artifacts, is explored in a separate study [Wu, 2024].

113 Overall, 2,089 cluster-heads, all topologically dissimilar to one another and to known  
114 inhibitors, were chosen for synthesis and testing. Of these, 1,521 were successfully synthesized  
115 (a fulfillment rate of 73%). Manual inspection (“manual-picked”) from among the better scoring

116 bins (-100.58 to -79 kcal/mol) accounted for 687 of these compounds, and another 1,292  
117 molecules were chosen based on rank alone (“auto-picked”), with 458 molecules occurring in both  
118 sets.

119 All molecules were initially tested at 200, 100, and 40  $\mu\text{M}$  concentrations for AmpC  
120 inhibition<sup>1,16,20</sup>. Of the 1,447 experimentally well-behaved molecules, 1,296 were among the top  
121 scoring 1% of the docked molecules, the same cut-off used in the 99 million molecule screen (the  
122 rest were spread out among lower ranks and were selected to test hit rate versus score  
123 dependence). Of these 1,296 compounds, 171 had an apparent  $K_i < 166 \mu\text{M}$ , based on the three-  
124 point inhibition numbers and assuming competitive inhibition (see below), while another 124 had  
125 apparent  $K_i$  values between 166 and 400  $\mu\text{M}$ . Concentration-response curves were measured for  
126 17 compounds across this potency range. The  $\text{IC}_{50}$  values from these full curves corresponded  
127 well to those predicted by the three-point inhibition numbers (**Extended Data Table 1, Extended**  
128 **Data Fig. 2**). For seven of the new inhibitors, each in a different chemotype family, we determined  
129 full  $K_i$  values and mechanism by Lineweaver-Burk analysis (**Extended Data Fig. 3**). All seven  
130 were competitive inhibitors, consistent with docking to the AmpC active site, with  $K_i$  values ranging  
131 from 0.7 to 4.6  $\mu\text{M}$  (**Extended Data Fig. 3**). Accordingly, we modeled all of the new inhibitors as  
132 competitive, consistent with the x-ray crystal structures determined for five of the new inhibitors,  
133 which were all observed to bind in the  $\beta$ -lactamase active site (**Fig. 1**). With this assumption,  $K_i$   
134 values ranged from 464 to 0.46  $\mu\text{M}^{24}$ , with substantial representation across this range of affinities  
135 (**Fig. 2**). All assays included 0.01% Triton X-100, diminishing the likelihood of artifact from  
136 colloidal aggregation<sup>18,25</sup>. For further confidence, 140 of the inhibitors were checked for particle  
137 formation by dynamic light scattering (DLS)<sup>25-27</sup>; no signs of colloid-like particle formation were  
138 detected among any of them at relevant concentrations (**Extended Data Table 2**).

139           **Docked versus crystallographic geometries.** To investigate how docking predicted  
140 geometries corresponded to experimentally-determined ligand poses, the structures of five of the  
141 new inhibitors were determined by x-ray crystallography, with resolutions varying from 1.6 to 2.9  
142 Å (**Extended Data Table 3**). Unambiguous electron density allowed us to confidently model the  
143 positions of the new inhibitors in the enzymes' active site. For **Z6615020275** (1.3 µM; **Fig. 1a**),  
144 **Z6615017782** (0.95 µM; **Fig. 1b**) and **Z6615017509** (0.86 µM; **Fig. 1c**), the docked and  
145 experimental structures superimposed with a 0.79, 0.97, and 3.14 Å root mean square  
146 deviation (RMSD) respectively, with the differences in position stemming from deviations of non-  
147 warhead groups binding distally in the site. For two weaker inhibitors, the crystal structures had  
148 larger deviations from the docking predictions. While the crystallographic pose of **Z8427841182**  
149 (36 µM) hydrogen-bonded with many of the same residues predicted in the docking pose, the  
150 crystallographic geometry was shifted in the site and the RMSD was high at 4.73 Å RMSD. This  
151 hydroxy-isoxazole, a close analog of the original 36 µM docking hit **Z6615146331** that had  
152 resisted facile crystallization (**Extended Data Table 1**), represents a previously unknown warhead  
153 for AmpC. Meanwhile, the crystallographic pose of the 323 µM **Z4462773688**, an unprecedented  
154 bicyclo-alkyl carboxylate, bound in a geometry flipped from that anticipated by docking, leading  
155 to an RMSD of 5.61 Å (**Fig. 1e**). **'6631** and **'3688** are two examples of the 44 inhibitors found in  
156 this campaign that sample not only novel topologies, but also novel warheads for AmpC.



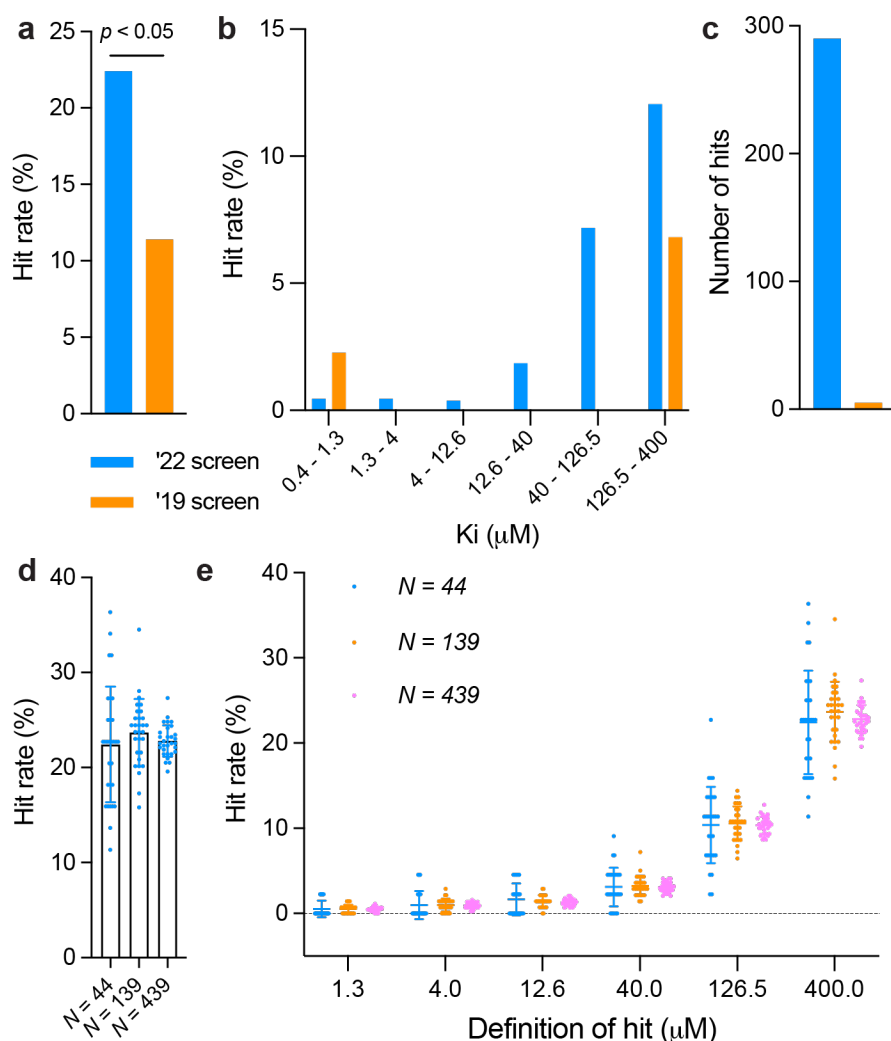
157  
158 **Fig. 1. Superposition of the crystallographic and docking poses of the new AmpC**  
159 **inhibitors.** Crystal structures (carbons in cyan) and docked poses (carbons in magenta) of the  
160 inhibitors. AmpC carbon atoms are in grey, oxygens in red, nitrogens in blue, sulfurs in yellow,  
161 chlorides in green, and fluorides in light blue. Hydrogen bonds are shown as black dashed lines.  
162 **a-c,** AmpC in complex with **Z6615020275** (r.m.s.d to crystal structure 0.79 Å,  $K_i$  2  $\mu$ M),  
163 **Z6615017782** (r.m.s.d = 0.97 Å, 1.5  $\mu$ M) and **Z6615017509** (r.m.s.d = 3.14 Å, 0.86 nM). The  
164 overlay of the crystal and docked poses are shown. **d-e,** AmpC in complex with **Z8427841182**  
165 (r.m.s.d = 4.73 Å, 36  $\mu$ M) and **Z4462773688** (r.m.s.d = 5.61 Å, 325  $\mu$ M). The docked poses (left  
166 panel), crystal poses (middle panel) and the overlay of the docked and crystal poses are shown  
167 (right panel).  
168

169 **Hit rates are higher from the larger vs the smaller library screens.** The overall hit rate  
170 (number experimentally active/number experimentally tested) from the 1.7 billion molecule  
171 docking screen was 22.4% (290 actives/1,296 high-ranking tested). This hit rate is significantly  
172 higher than that from 99 million molecule docking screen, which was 11.4% ( $p$ -value < 0.05) (**Fig.**  
173 **2a**). The hit rate difference stands out even more strongly when considered across affinity ranges.



174 Most of the actives from the 99 million molecule screen had apparent  $K_i$  values between 126.5  
175 and 400  $\mu\text{M}$  (**Fig. 2b**), with one inhibitor found in the 1 to 10  $\mu\text{M}$  range, and none found in the  
176 intermediate ranges. Conversely, from the 1.7 billion library each half-log affinity bin is well-  
177 populated by active molecules. The higher hit rate from the larger library is consistent with the  
178 idea that as the virtual libraries grow, ever more plausible molecules are fortuitously sampled and  
179 prioritized by molecular docking.

180 **Hit rate variability and ligand affinity ranges.** While hit rate is a fair way to compare the  
181 two screens, naturally, the raw number of hits was far greater from the larger library (290 active  
182 from 1.7 billion screened versus 5 actives from 99 million screened, **Fig. 2c**), where 29-fold more  
183 high-ranking molecules were tested. Qualitatively this explains why all half-log affinity bins were  
184 well-populated from the larger library, whereas this was more hit-and-miss when we only tested  
185 44 molecules (**Fig. 2b**). To quantify how hit rate varies with the number experimentally tested, we  
186 randomly pulled sets of 44, 139 and 439 molecules from the 1,296, each 30 times, and asked  
187 how this affected hit rate. When only selecting 44 molecules—the number tested in the smaller  
188 library campaign—hit rates varied from 11% for one unlucky draw to 36% for a lucky one. Pulling  
189 sets of 439 molecules 30 times, the hit rate only varied from 20% to 27%. As the number of  
190 molecules experimentally tested increased, the standard deviation in hit rates decreased from  
191 6.1% to 3.5% to 1.7% (**Fig. 2d**). This variability was even starker when plotted by affinity bin; for  
192 instance, it was not until set size rose to 439 molecules tested that the highest affinity molecules  
193 were reliably sampled (**Fig. 2e**). Re-analyzing previous campaigns against the  $\sigma 2$  and dopamine  
194 receptor<sup>1,4</sup>, where around 500 molecules were experimentally tested, similar variability was seen  
195 in both hit rates and in sampling of the high-affinity docking hits, which for  $\sigma 2$  were in the low  
196 nanomolar range (**Extended Data Fig. 4**).



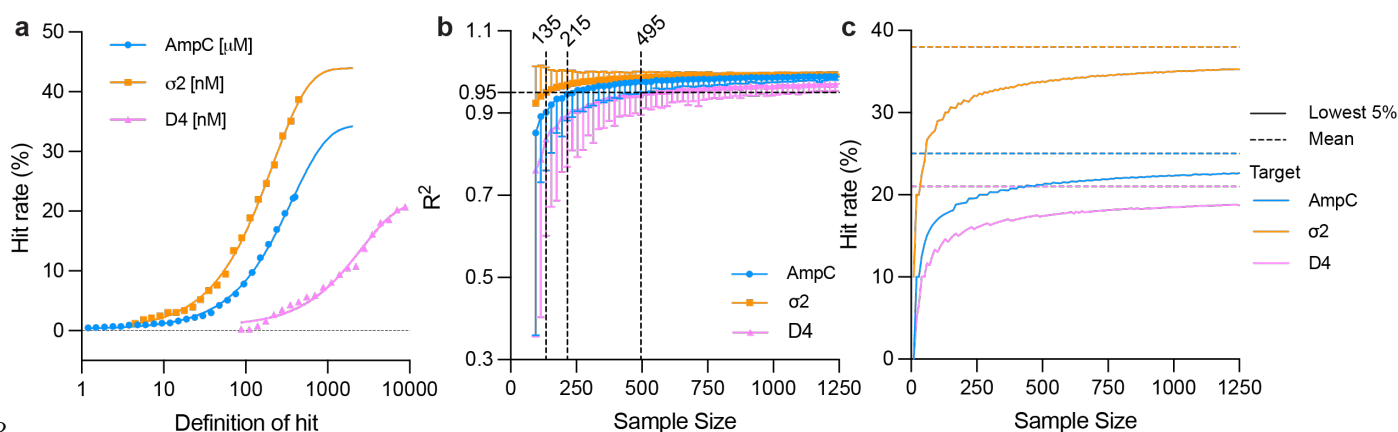
197  
 198 **Fig. 2. Larger-scale docking and testing increases hit rates and reduces uncertainty.** **a**, The  
 199 hit rates (number of actives/total tested) of the **1.7 Billion** screen (blue bar) versus the **99 Million**  
 200 screen (orange bar). **b**, Hit rates by different affinity bins in '22 screen and '19 screen. **c**, Number  
 201 of hits (number of actives) of the **1.7 B** screen (blue bar) versus the **99 M** screen (orange bar). **d**,  
 202 The impact of randomly purchasing 44, 139, 439 molecules out of 1,296 molecules for testing on  
 203 hit rates. Each sample size is randomly drawn 30 times and the resulting hit rates were plotted.  
 204 The error bars represent SDs of the hit rates. The hit rates are  $22.42 \pm 6.08\%$  ( $N = 44$ ),  $23.67 \pm$   
 205  $3.54\%$  ( $N = 139$ ) and  $22.80 \pm 1.65\%$  ( $N = 439$ ). **e**, The impact of randomly purchasing 44, 139,  
 206 439 molecules out of 1,296 molecules for testing on hit rates with different affinity cutoffs. Each  
 207 sample size is drawn 30 times and the resulting hit rates were plotted. The error bars represent  
 208 SDs of the hit rates.  
 209

210 These results suggest that both hit rates and affinities in docking screens may be  
 211 unreliable when only dozens of molecules are tested, as is common in the field. To quantify how  
 212 many molecules should be tested to report stable hit rates and affinity ranges, we drew on the

213 observation that when large numbers of molecules are experimentally tested for AmpC, and for  
214 the  $\sigma 2$  and the dopamine D4 receptors, there is an exponential relationship between affinity and  
215 hit rate, something also seen in high-throughput screens<sup>28</sup>. For the top-ranking 1% of docked  
216 molecules from each campaign, we modeled hit rates ( $y$ ) and hit affinities ( $x$ ) with an exponential  
217 function  $y = b(1 - e^{-cx})$  for each of AmpC,  $\sigma 2$  and D4 (**Fig. 3a**). This functional form fit the  
218 distribution of affinities for the 1,296 molecules tested for AmpC, 327 for  $\sigma 2$  and 371 for D4 (all  
219 top 1% ranking molecules) with  $R^2$  values of 0.998, 0.998, and 0.985, respectively. As smaller  
220 sets are drawn from the full sets, variability rises (**Fig. 2**). Beginning with a sample size of 1,296,  
221 sampling was stepwise reduced by 20 molecules in a bootstrapping manner, repeating this 1,000  
222 times to evaluate divergence (**Fig. 3b**). By ~495 molecules, the average  $R^2$  of D4 curves falls to  
223 0.95, a point on all three curves where we began to see the meaningful divergence the fit achieved  
224 over the full range of compounds plotted. This same  $R^2$  occurs at 215 and 135 molecules for  
225 AmpC and  $\sigma 2$ , respectively, reflecting a relationship that is inversely proportional to the hit rate  
226 for each target among the top-scoring 1% of the docked molecules (22.4% hit rate for AmpC,  
227 38.7% for  $\sigma 2$  and 20.8% for D4). In these targets, testing fewer than these several hundred  
228 compounds degrades the correlation of affinity with hit rate, which is useful for planning how many  
229 compounds should be tested. For targets with relatively high hit rates, this suggests that over a  
230 hundred molecules should be experimentally tested for confident hit rates and affinity ranges from  
231 molecular docking. For targets where one might expect lower hit rates, even more compounds  
232 would need to be tested for confident results.

233 To explore this further with a focus on hit-rate variability, we simulated random draws using  
234 the AmpC,  $\sigma 2$ , and D4 experimental hit rates from their high-ranking compounds. One hundred  
235 thousand bootstrap iterations were performed for sample sizes ranging from 10 to 1250  
236 compounds in increments of 10 and we considered the mean and lower bound for a single-sided  
237 95% confidence interval at different numbers of compounds tested (**Fig. 3c**). The solid curves

238 reflect the 95% likelihood that the hit rate will be at a certain level or higher. While the average hit  
 239 rate over all simulations remains unchanged, the variability increases as the number of molecules  
 240 tested drops, and so does one's confidence that the observed hit rate reflects the true hit rate  
 241 based on the overall docking rankings. This again suggests over 100 molecules may be a sensible  
 242 minimum for experimental testing in large library virtual screens, even for campaigns from which  
 243 one expects relatively high hit rates. Encouragingly, while both the affinity ranges and the hit rates  
 244 for the screens against AmpC,  $\sigma$ 2 and D4 differ substantially, the functional form relating hit affinity  
 245 and hit number was the same and led to similar predictions for the minimum number of molecules  
 246 to test for all three targets. This lends itself to predicting how many molecules would be found in  
 247 different affinity ranges should one choose to test more molecules, a point to which we will return.



248  
 249 **Fig. 3. Several hundred compounds should be tested in ultra-large docking campaigns. a,**  
 250 For the top-ranking 1% of the docked molecules, the relationship between hit affinity and hit rates  
 251 can be fit with an exponential plateau model  $y = b(1 - e^{-cx})$  with  $y$  represents the hit rate,  $x$  is  
 252 minimum affinity to be classified as a hit (for AmpC, the unit is in micromolar and for  $\sigma$ 2 and D4,  
 253 the unit is in nanomolar),  $b$  is the maximal hit rate. The fit maximal hit rates are 34.5% for AmpC  
 254 with an  $R^2$  of 0.998, 43% for  $\sigma$ 2 receptor with an  $R^2$  of 0.998, and 20.8% for D4 with an  $R^2$  of 0.985.  
 255 **b,** The impact of sub-sampling on the  $R^2$  of the fit. From among the top-ranking 1% of the docked  
 256 molecules, 1,295 (AmpC, blue), 327 ( $\sigma$ 2, orange) and 371 (D4, pink), each subsample is  
 257 bootstrapped 1,000 times and fit with the parameters derived from the entire dataset. The  $R^2$   
 258 values are plotted with the symbols indicating the average and the error bars indicating the  
 259 standard deviations of the  $R^2$ . A dashed line of  $R^2 = 0.95$  is labeled. The sample sizes at which  
 260 the average  $R^2$  value reaches 0.95 are labeled. For  $\sigma$ 2, the sample size is 135, for AmpC, it is  
 261 215; and for D4, it is 495. **c,** Mean and 95% confidence interval for hit rate in relation to sample  
 262 size for AmpC,  $\sigma$ 2 and D4. The dashed lines show the mean hit rate from the compounds in the  
 263 top 1% by docking score, and the solid line shows the boundary of a single-sided 95% confidence  
 264 interval from 100,000 bootstrap iterations. Hits are defined as 400  $\mu$ M affinity or better for AmpC,  
 265 677.5 nM or better for  $\sigma$ 2 and 10  $\mu$ M or better for D4.

266

267           **Multiple novel chemotypes discovered.** Only molecules topologically dissimilar from  
268 known AmpC inhibitors, and topologically diverse among each other, were selected for synthesis  
269 and testing. Since topological diversity can emerge from rearrangements and changes that leave  
270 core pharmacophores intact, we also visually inspected inhibitors for novelty. We prioritized these  
271 by two criteria: molecules that sampled new scaffolds, and molecules that explored a new  
272 warhead for binding in the crucial oxyanion recognition site of AmpC (Extended Data **Fig. 5**). For  
273 instance, **Z6615021877** and **Z6722203632** introduce tetrazolone and tetrazole anionic warheads,  
274 respectively, both of which were previously unknown for AmpC. **Z2607647274** and **Z4173922012**  
275 employ cycloalkyl carboxylate and tricyclo-heptane carboxylate as their warheads. Meanwhile,  
276 **Z2610488449**, which utilizes a novel urea linker scaffold, achieves a high affinity of 12  $\mu\text{M}$ . The  
277 affinity of this scaffold was readily optimized to 4  $\mu\text{M}$ , marking it among the most effective AmpC  
278 inhibitors that does not rely on a sulfonamide linker.

279           **Docking score predicts hit rate.** In earlier studies against the dopamine D4 and  $\sigma_2$   
280 receptors, we had found that docking score correlated to experimental hit rate, generating a well-  
281 behaved sigmoidal curve that plateaued at a maximum hit rate once more favorable docking  
282 scores were reached<sup>1,4</sup>. While these curves suggested an unexpected ability to categorize  
283 molecules as ligands, both receptors have unusually well-formed, buried binding sites. Moreover,  
284 the plateauing of the score vs. hit rate curve suggests a limitation in even our ability to *categorize*,  
285 far less rank-order. To investigate how docking might predict binding in a more solvent-exposed,  
286 historically more difficult binding site, we re-explored this relationship for AmpC. Docked  
287 molecules were not only selected from among the very best docking energies, as is typical in  
288 virtual screening, but also from mediocre and unfavorable docking scoring ranges. Molecules  
289 were picked from among 16 scoring “bins” beginning at the most favorable DOCK3.8 scores (-  
290 100.58 kcal/mol for AmpC) down to -28 kcal/mol. The top 1% of the docking-ranked library

291 extends down to -72 kcal/mol scores, and ranks fall off steeply from there such that by -28 kcal/mol  
292 49% of the 1.7 billion molecule library has been sampled. More than 50 molecules per bin were  
293 selected from the -100.58 to the -60 kcal mol<sup>-1</sup> bin, and for scores worse (less negative) than -60,  
294 more than 20 molecules were tested per bin. Molecules were selected strictly by numerical rank  
295 at the beginning of each bin. These were tested for AmpC inhibition as above and docking score  
296 was plotted against experimental hit rate (number active/number tested) (**Fig. 4a**).

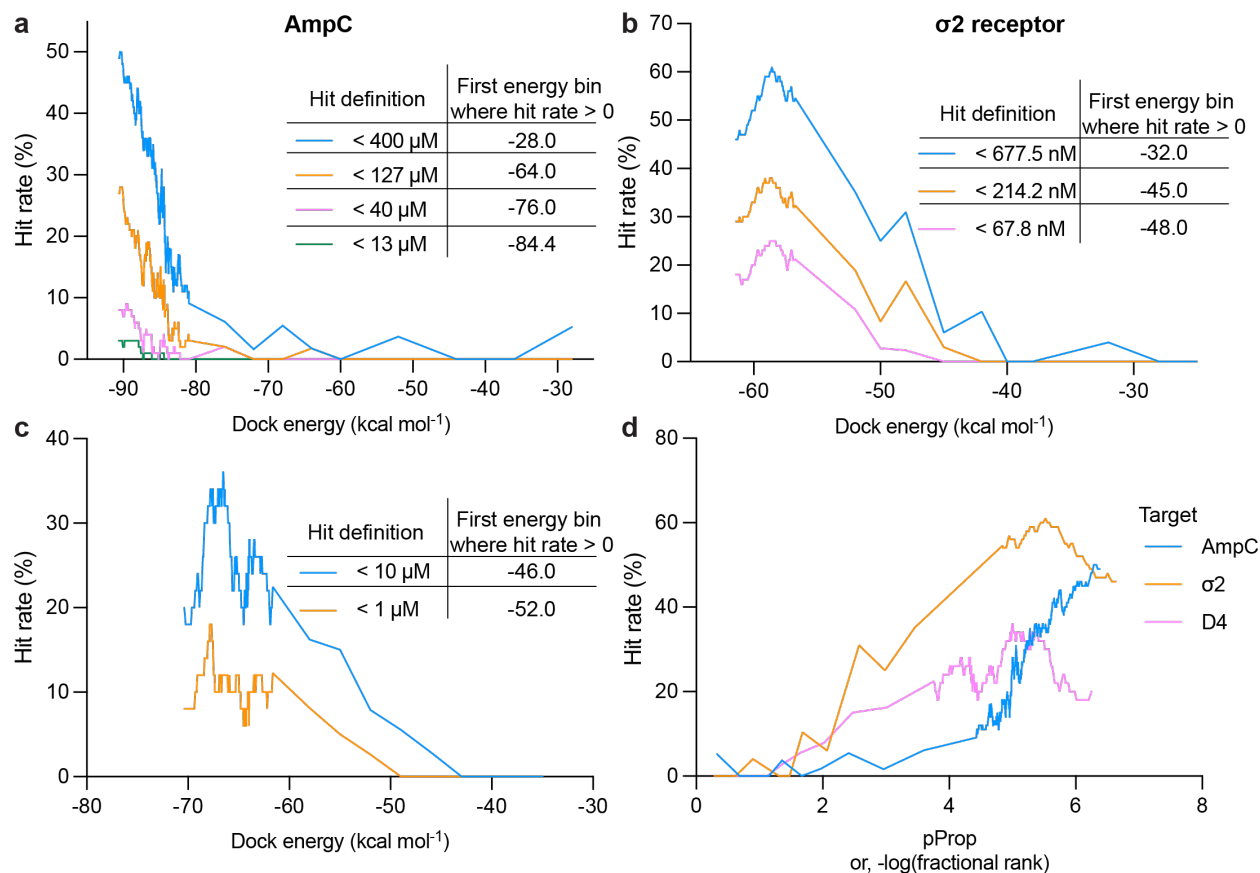
297 Notably, hit rates fell monotonically as scores worsened (**Fig. 4a**, blue curve). This  
298 resembles what had been previously observed for the  $\sigma$ 2 and dopamine receptors<sup>1,4</sup>, except that  
299 here we do *not* observe a hit rate plateau; hit rates begin at a maximum at the best docking scores  
300 and fall steadily as scores worsen. The difference between the AmpC results and the plateaus  
301 observed previously is that for AmpC we were careful to from the beginning exclude a small  
302 fraction of likely artifacts that concentrate among the very top scoring molecules<sup>14</sup> (Extended Data  
303 **Fig. 1**).

304 To investigate how the *affinities* of docking actives also track with docking rank, we plotted  
305 docking score versus hit rate in the 400, 127, 40, and 13  $\mu$ M ranges (**Fig. 4a**, orange, pink, and  
306 green curves). As for the behavior of the overall set of actives, the hit rates in each affinity-range  
307 rose steadily as score improved. Intriguingly, the more potent inhibitors appear at better scores  
308 than the less potent ones, with those in the 127  $\mu$ M or better tranche beginning to appear at scores  
309 of -64, those in the 40  $\mu$ M or better tranche appearing only past -76, and the most potent inhibitors  
310 only appearing at the -85 bin. This hints at docking score correlating with gross categorical ranking  
311 of affinity, something that has not apparent from smaller studies, nor even expected<sup>29,30</sup>. To  
312 explore generality, we undertook the same analysis with the docking campaigns against the  $\sigma$ 2  
313 receptor and dopamine D4 receptor, where hundreds of molecules were tested across docking  
314 ranks that ranged from high to mediocre to poor, as in this study. While the  $\sigma$ 2 and dopamine

315 receptor docking hits were more potent than the AmpC hits, typically in the nM range, the same  
316 patterns emerged—the most potent ligands appear at better (more negative) docking scores than  
317 did the mid-potency ligands, which appear at better scores than did those with the lowest affinity  
318 threshold (**Fig. 4b-c**). Admittedly, the relationship between docking score and affinity is mostly  
319 categorical, but it appears to rank molecules better than simple binary classification as binders or  
320 non-binders, with more potent ligands more concentrated in better-scoring regions. As loose as  
321 these correlations are, they may support a predictive relationship between docking score and  
322 affinity category (high, medium, or low), at least when tested at scale. This would warrant a  
323 renewed emphasis on improving the field’s scoring functions and offer a metric against which they  
324 might be tested.

325

326 To compare the hit rate curves for the three targets, we plotted the negative logarithm of  
327 the rank percent (“pProp”) for the dopamine and  $\sigma_2$  receptors, and for AmpC (**Fig. 4d**). A pProp  
328 of 3 denotes a compound occupying the top 0.1% scoring region, a pProp of 4 the top 0.01%, and  
329 so on; plotting rank avoids scoring offsets among the targets. The hit rate curve of the most  
330 permissive hit definition for each target is plotted against the pProp. The D4 and  $\sigma_2$  curves align  
331 well, peaking around a pProp of 5, with the plateau occupying the region from 4 to 6 (top in 10,000  
332 to top in 1,000,000), while the AmpC curve is slightly right shifted, peaking above 6 and not  
333 suffering from a plateau. These curves allow one to quantify the parts of the docking scoring range  
334 where most hits are likely to be found. For the D4 and  $\sigma_2$  receptors, it also alerts one to the danger  
335 of over-emphasizing the very best ranked molecules where those that cheat the scoring function  
336 concentrate, absent controls for them<sup>14</sup>. As docking and virtual screening libraries climb into the  
337 tens-of-billions of molecules<sup>5,21</sup>, this concern will become more pressing.



338  
 339 **Fig. 4. Hit rate of experimentally tested compounds plotted against DOCK scores with**  
 340 **different affinity cutoffs. a,** The AmpC hit rates of 1,292 auto-picked compounds using four  
 341 different affinity cutoffs, < 400, 137, 40 and 13  $\mu\text{M}$ , are plotted against DOCK scores. **b,**  $\sigma 2$   
 342 receptor hit rates of 484 compounds plotted against DOCK scores with three different affinity  
 343 cutoffs: < 667.5, 241.2, 67.8 nM. **c,** Dopamine D4 hit rates of 549 compounds plotted against  
 344 DOCK scores with two different affinity cutoffs: <10 and <1  $\mu\text{M}$ . **d,** Rescaling the hit rate curves  
 345 of the three targets by the  $\log_{10}$  of fractional rank in the library. For each target, the most  
 346 permissive hit definition is used.

347  
 348  
 349  
 350  
 351

## Discussion

352 In the last five years, the number of molecules readily accessible for ligand discovery has  
 353 expanded 10,000-fold. Anecdotally, this has led to ligands with improved activity from library  
 354 docking. How true this is, however, has not been quantified in apples-to-apples comparisons of  
 355 smaller vs. larger libraries. Several other inferences from large library docking screens have also  
 356 not been quantified, such as that testing more high-ranking molecules yields correspondingly



357 more ligands, or that as docking score improves so too does hit rate and perhaps even affinity.  
358 Here, we begin to test these ideas experimentally; five key observations emerge<sup>1,14</sup>. **First**,  
359 comparing a docking screen of 99 million molecules to one of 1.7 billion molecules, against the  
360 same target, hit rates improved with library size, as did the potency of the inhibitors. Multiple new  
361 chemotypes were discovered, not previously observed as AmpC inhibitors. **Second**, consistent  
362 with the idea that there are many more ligands to be discovered than are being prioritized, the  
363 number of new inhibitors found scaled almost linearly with the number of top-ranking molecules  
364 tested; experimentally testing 30-fold more molecules led to the discovery of 50-fold more  
365 inhibitors. **Third**, to determine reliable docking statistics from a large library screen, one must also  
366 *experimentally test* at scale. When only a handful of molecules are tested, as is common in  
367 docking, statistics of hit-rates and maximal affinities will have large error ranges. This study  
368 suggests that typically several hundred molecules should be tested for docking statistics to be  
369 trustworthy. **Fourth**, in contrast to earlier studies where we saw hit rates plateau above a certain  
370 docking score<sup>1,4</sup>, here no plateau was observed in the hit rate vs. docking score curve—hit rates  
371 continued to climb monotonically and essentially linearly as score improves. This was also true  
372 for the dopamine and  $\sigma_2$  receptors on re-analysis after removing their high-ranking artifacts. While  
373 more studies are necessary, this observation supports the idea that as libraries grow, hit rates  
374 and hit affinities will improve, as long as high-ranking docking artifacts can be removed or avoided.  
375 **Finally**, a loose, categorical correlation between docking score and ligand affinity was observed  
376 for AmpC, and on re-analysis also for the  $\sigma_2$  and dopamine D4 receptor campaigns where  
377 sufficient molecules were also tested across the scoring range to support this analysis<sup>1,4</sup>. While  
378 this correlation remains loose and only by relative affinity category (e.g., strong, mediocre, weak),  
379 it may suggest that further optimization of docking scoring functions will allow the field to  
380 distinguish not only binders from non-binders, but also categorically rank them by activity,  
381 something we and others have long discounted<sup>29,30</sup>.

382           Several caveats should be aired. Most importantly, the monotonic improvement of hit rate  
383 with docking score, and the loose categorical correlation between affinity and score, have only  
384 been observed in three systems. This merits investigation in other targets, ideally using other  
385 scoring functions, at scale. Current community tests of docking methods, such as CACHE<sup>31</sup>, may  
386 offer a forum for doing so. Methodologically, we note that for less than 10% of the molecules  
387 reported here were full IC<sub>50</sub> curves determined. While these correlated well with inferred IC<sub>50</sub> and  
388 K<sub>i</sub> values based on three concentration point inhibition, such affinities must be considered  
389 approximate.

390           These caveats should not obscure the major observations of this study. Against the same  
391 target, docking a 20-fold larger library led to improved hit rates and affinities, consistent with  
392 theoretical simulations<sup>14</sup>. Similarly, as more high-ranking molecules are tested, more ligands are  
393 found, supporting the idea that most true ligands in the new ultra-large libraries remain to be  
394 tested (we suffer from an embarrassment of riches). Once we correct for high-ranking docking  
395 artifacts, hit rate rise monotonically with docking score. More tentatively, a correlation between  
396 affinity and score also appears at scale. How this holds up will depend on further testing, but even  
397 now these results support continued investment in library growth and methods that can exploit it.  
398 While brute force docking, of the sort described here, has been able to address a 1000-fold  
399 increase in library size, to go up another thousand-fold, into the trillions of molecules, seems  
400 beyond it, and more guided sampling of chemical space may be required<sup>5,11,32,33</sup>. To support such  
401 efforts, we are making available the identity, docking scores, and experimental activities of each  
402 of the 1521 molecules tested in the enzyme assay (**SI Table 1**), and extensive docking score and  
403 pose information from the full library screen (<https://lsd.docking.org>). What this study does  
404 suggest is that efforts to sample from the supra-trillion molecule space should be worthwhile.

405

## 406 **Data and code availability**

407 The compounds docked in this study are freely available from the ZINC20 and  
408 ZINC22 databases, <https://zinc20.docking.org> and <https://cartblanche22.docking.org>. All  
409 compounds tested can be purchased from Enamine. Compound information including  
410 their ZINC ID, SMILES, DOCK score, ranking, and affinity can be found in **SI Table 1**.  
411 The synthetic procedures and purity information for the hits can be found in the **SI Data**  
412 **2** and **SI Table 3**. Extensive docking-related files can be found at <https://lsd.docking.org>.  
413 DOCK3.8 is freely available for non-commercial research at  
414 <https://dock.compbio.ucsf.edu/DOCK3.8/>. A web-based version is available without  
415 restriction at <https://blaster.docking.org/>. X-ray structures and maps are available in the  
416 Protein Data Bank under accession numbers PDBID 9C81 (Z4462773688), PDBID 9C6P  
417 (Z6615017509), PDBID 9C83 (Z8427841182), PDBID 9C84 (Z6615020275), and PDBID  
418 9C8J (Z6615017782) respectively.

419

## 420 **Acknowledgements**

421 Supported by US National Institutes of Health (NIH) grants R35GM122481 (to BKS) and  
422 GM71896 (to JJI), and a Damon Runyon Postdoctoral Research Fellowship (FL). We thank  
423 ChemAxon for JChem, OpenEye Scientific software for OEChem and Omega2, Molecular  
424 Networks for Corina, Molinspiration for Mitools, and Schrodinger LLC for the Maestro suite. We  
425 thank George Meigs and James Holton for their assistance at Beamline 8.3.1 at the Advanced  
426 Light Source, operated by UCSF with NIH grants R01 GM124149 for technology development  
427 and P30 GM124169 for beamline operations, and the Integrated Diffraction Analysis  
428 Technologies program of the US Department of Energy Office of Biological and Environmental  
429 Research. We thank Karthik Srinivasan for his assistance on data collection. The Advanced Light

430 Source (Berkeley, CA) is a national user facility operated by Lawrence Berkeley National  
431 Laboratory on behalf of the US Department of Energy under contract number DE-AC02-  
432 05CH11231, Office of Basic Energy Sciences.

433

434 **Author Contributions:** FL conducted the docking screens and the ligand optimization  
435 assisted by SV and advised by BKS. FL and IG conducted the *in vitro* enzymatic assays, with  
436 early assistance from SV. FL determined the structures by X-ray crystallography, with assistance  
437 from VB, XX, advised by JF. FL and OM did the analysis with advice from MS. Aggregation studies  
438 were conducted by KFV and IG. JJI developed and prepared the make-on-demand library  
439 assisted with large library docking strategies. DSR and YSM supervised compound synthesis of  
440 Enamine compounds purchased from the ZINC22 database and the 46 billion catalog library.

441

442 **Declaration of Interests:** BKS is a founder of Epiodyne, Inc, BlueDolphin, LLC, and Deep  
443 Apple Therapeutics, Inc., serves on the SAB of Schrodinger LLC and of Vilya Therapeutics, on  
444 the SRB of Genentech, and consults for Hyku Therapeutics. JJI co-founded Deep Apple  
445 Therapeutics Inc. and BlueDolphin LLC. JSF is a consultant for, has equity in, and receives  
446 research support from Relay Therapeutics.

447

448

449

450

451

452

453

454

455

## 456 **Methods**

457 **Large-scale docking.** The campaign used the structure in PDB 1L2S. Three Q120 conformations  
458 were modeled based on the X-ray density of 3FKW using qFit-3.0, with an occupancy of 0.49,  
459 0.34 and 0.17<sup>34</sup>. The occupancy of the alternative conformations was converted into an additional  
460 energy term and incorporated in the DOCK scoring function as described previously<sup>35</sup>. The protein  
461 structure was protonated using Reduce<sup>36</sup>. Energy grids for the different energy terms of the  
462 scoring function were pre-generated--van der Waals term based on the AMBER force fields using  
463 CHEMGRID<sup>37</sup>; Poisson-Boltzmann-based electrostatic potentials using QNIFFT73<sup>38,39</sup>; context-  
464 dependent ligand desolvation was calculated using SOLVMAP<sup>40</sup>. The volume of the low dielectric  
465 and the desolvation volume was extended out 2.0 and 0.25 Å. The thiophene carboxylate inhibitor  
466 solved in PDB 1L2S was used to generate matching spheres, which are later used by the docking  
467 software to fit pre-generated ligands' conformations into the small molecule binding sites<sup>41</sup>. The  
468 resulting docking set-ups were evaluated for its ability to enrich known AmpC ligands over  
469 property-matched decoys. Decoys are theoretical non-binders to the receptor as they are  
470 topologically dissimilar to known ligands but retain similar physical properties. We curated 31  
471 AmpC ligands based on their dissimilarity among themselves. 2,480 decoys were generated by  
472 using the DUDE-Z pipeline<sup>42</sup>. The docking set-up can rank ligands over decoys with a logAUC of  
473 28.5 with the majority of the ligands recapitulating their experimental poses. For docking against  
474 1.7-billion molecules, each molecule from the ZINC22 database<sup>43</sup> was sampled in about 3,822  
475 orientations and 875 conformations by using DOCK3.8<sup>41</sup>. Overall, over 1841 trillion complexes  
476 were sampled and scored, spending 2,129,230 core hours, or about a month on a 3,000 core  
477 cluster, using DOCK3.8<sup>41</sup>.

478

479 **Hit-picking strategy.** To increase novelty, high-ranking molecules with scores down to -79.25  
480 (99,277 molecules), and molecules from different energy bins (25,000 from -76, -72, -68, -64 and

481 -60 bins and 5,000 from -52, -44, -36 and -28 bins), summed to 244,277 molecules, were filtered  
482 to exclude those similar to 237 previously known ligands. A  $T_c$  cutoff of 0.5 was used; no molecule  
483 more similar than this value was allowed, removing 9,712 molecules. We also filtered out  
484 molecules that buried too many uncompensated polar groups—while DOCK3.8 penalizes for  
485 desolvation, we find that these artifacts can nevertheless occur. Using LUNA 1,024-length binary  
486 fingerprints<sup>23</sup>, molecules that had more than 1 hydrogen bond donor and more than 6 hydrogen  
487 bond acceptors that were not compensated with polar interactions to the protein were removed;  
488 40,687 molecules were filtered-out at this step. This left 193,878 for further processing. For  
489 autopicking, these molecules were clustered for self-similarity using an ECFP4  $T_c = 0.32$ , resulting  
490 in 80,767 cluster heads.

491  
492 Most of the molecules tested were “autopicked” based on docking rank. With almost all of the  
493 high-ranking molecules being negatively charged, we wanted to ensure that their representation  
494 as anions at pH 7.4 was likely. We used JChem to calculate the distribution of protonation states  
495 of the high-ranking cluster heads and compared this to the dominant state represented in their  
496 docked poses (multiple protonation states of a molecule can be docked). Only when the  
497 calculated dominant charge state matched with that of the docked pose, and the species is  
498 calculated to be more than 80% anionic, was the molecule accepted for autopicking, which left  
499 56,814 molecules. Molecules were picked based on their docking ranks across different affinity  
500 bins, selecting 1,274 molecules for synthesis and testing.

501  
502 For manual picking from the different energy bins, all cluster heads were again filtered for  
503 interactions using LUNA, seeking molecules that formed hydrogen bonds with backbone of A318,  
504 that made pi-pi interactions with Y221, and that made at least two more interactions with the  
505 binding pocket (i.e. hydrogen bonds with N152, N346, G320, S212, R204, Q120, cation-pi with  
506 K315, K67, or pi-pi interaction with Y150). The molecules that passed these filters were re-

507 clustered at a  $T_c = 0.32$ ; cluster heads were visually inspected and prioritized. The rest of the  
508 high-scoring cluster heads were also manually inspected seeking new interesting chemotypes. A  
509 total of 687 were prioritized manually, slightly less than half of the molecules that were synthesized  
510 and tested.

511  
512 **AmpC enzymology.** All candidate inhibitors were dissolved in DMSO at 20 mM, and more dilute  
513 DMSO stocks were prepared as necessary so that the concentration of DMSO was held constant  
514 at 1% v/v in 50 mM sodium cacodylate buffer, pH 6.5. AmpC activity and inhibition was monitored  
515 spectrophotometrically using either CENTA or nitrocefin as substrates. All assays included 0.01%  
516 Triton X-100 to reduce compound aggregation artifacts. Active compounds were further  
517 investigated for aggregation by dynamic light scattering (DLS) and by detergent-dependent  
518 inhibition of the counter-screening enzyme malate dehydrogenase.

519  
520 For initial screening, the docking hits were diluted such that final concentrations in the reaction  
521 buffer was 200  $\mu\text{M}$ , 100  $\mu\text{M}$ , and 40  $\mu\text{M}$ . In these assays, two widely-studied AmpC substrates  
522 were used, depending on availability, CENTA<sup>44</sup> and nitrocefin<sup>16</sup>. The first was tested at an [S]/Km  
523 ratio of 1.81 (Km CENTA 27.6  $\mu\text{M}$ ; [S] = 50  $\mu\text{M}$ ) and the second was tested [S]/Km ratios of  
524 0.556 (Km nitrocefin 180  $\mu\text{M}$ ; [S] = 100  $\mu\text{M}$ ) and 0.156 ([S] = 28  $\mu\text{M}$ ). The colorimetric assay was  
525 converted to a medium throughput manner using a BMG Labtech CLARIOstar. Substrate (CENTA  
526 ( $\text{EC}_{50} = 27.6 \mu\text{M}$ ) or nitrocefin ( $\text{EC}_{50} = 180 \mu\text{M}$ )) and protein were injected into buffer containing  
527 the putative inhibitor, followed by rate measurement for 50 seconds in 96-well format.  $\text{IC}_{50}$  values  
528 reflect the percentage inhibition fit to a dose-response equation in GraphPad Prism with a Hill  
529 coefficient set to one ( $f(x) = \max - \frac{\max - \min}{1 + \frac{x}{\text{IC}_{50}}}$ ). The  $K_i$  was calculated using the Cheng-Prusoff  
530 equation ( $K_i = \frac{\text{IC}_{50}}{1 + \frac{[\text{S}]}{K_m}}$ ). For 18 of the more potent compounds, based on the initial three

531 concentration-point results, full dose response curves were measured, and for another eight full  
532 Ki values were measured and calculated using Lineweaver-Burk plots.

533  
534 **AmpC crystallization, data collection and structure determination.** AmpC crystallization was  
535 carried out as previously described<sup>16</sup>. Briefly, co-crystals of AmpC and inhibitors were grown by  
536 vapor diffusion in hanging drops equilibrated over 1.7 M potassium phosphate buffer (pH 8.7)  
537 using microseeding. The initial concentration of protein in the drop was 6 mg/mL and the  
538 concentration of the inhibitor was 0.5 mM. The inhibitor was added to the crystallization drop in a  
539 4% DMSO, 1.7 M potassium phosphate buffer (pH 8.7) solution. Crystals appeared within 3–5  
540 days after equilibration at 23°C.

541 Data were measured from a single crystal per complex on the Beamline 8.3.1 of the Berkeley  
542 Advanced Light Source, with wavelength 1.11583 Å at 100 K. Before data collection, co-crystals  
543 of AmpC were immersed in a cryoprotectant solution of 20% sucrose, and 1.7 M potassium  
544 phosphate (pH 8.7) for about 20 s and then flash-cooled in liquid nitrogen. The structures were  
545 solved by molecular replacement with PHENIX<sup>45</sup> using PDB 1L2S as the search model. Structure  
546 refinement was carried out with PHENIX and COOT<sup>46</sup>. MolProbity<sup>47</sup> was used for validation  
547 (**Extended Data Table 3**); structural figures were prepared using ChimeraX<sup>48</sup>.

548 **Hit rate curves.** To obtain hit rate curves, the experimentally tested molecules for each target  
549 (AmpC, the  $\sigma$ 2 and dopamine D4 receptors) were ordered by increasing DOCK score. A rolling  
550 window was passed over the list, calculating the hit rate as the percentage of molecules with  
551 experimentally determined affinity equal to or better than the hit definition, and the DOCK score  
552 as the average for the window. A window size of 100 was used for AmpC and  $\sigma$ 2, and a window  
553 of 50 for D4 receptor. For all three targets, molecules were picked from both within and outside  
554 of what would typically be considered high-ranking regions. The rolling window was stopped for



555 those scores outside the high-ranking region since discrete score bins were used in the hit-picking  
556 of these likely non-binders. The scores at which the rolling window was stopped are -78 for AmpC,  
557 -52.5 for  $\sigma 2$  and -60 for D4. For the pProp rescaling, the same strategy was used, but the DOCK  
558 scores were transformed to fractional rank based on the observed score distribution. The negative  
559 base 10 logarithm of the fractional rank is then reported, termed “pProp”.

560 **Hit rate modelling.** For sampling hit rate variability in relation to sample size, we used sample  
561 sizes for 10 to 1250 in jumps of 10. For each sample size, we picked 100,000 random samples  
562 of the uniform distribution [0, 1]. The hit rate of the sample was then defined as the number of  
563 observations with equal to or lower than the observed experimental hit rate for that target. A  
564 single-sided 95% confidence interval is built by taking the boundary value between the top 95%  
565 observed hit rates and the bottom 5%.

566

## 567 References

- 568 1 Lyu, J. *et al.* Ultra-large library docking for discovering new chemotypes. *Nature* **566**, 224-  
569 229, doi:10.1038/s41586-019-0917-9 (2019).
- 570 2 Gorgulla, C. *et al.* An open-source drug discovery platform enables ultra-large virtual  
571 screens. *Nature* **580**, 663-668, doi:10.1038/s41586-020-2117-z (2020).
- 572 3 Stein, R. M. *et al.* Virtual discovery of melatonin receptor ligands to modulate circadian  
573 rhythms. *Nature* **579**, 609-614, doi:10.1038/s41586-020-2027-0 (2020).
- 574 4 Alon, A. *et al.* Structures of the sigma(2) receptor enable docking for bioactive ligand  
575 discovery. *Nature* **600**, 759-764, doi:10.1038/s41586-021-04175-x (2021).
- 576 5 Sadybekov, A. A. *et al.* Synthon-based ligand discovery in virtual libraries of over 11 billion  
577 compounds. *Nature* **601**, 452-459, doi:10.1038/s41586-021-04220-9 (2022).
- 578 6 Fink, E. A. *et al.* Structure-based discovery of nonopioid analgesics acting through the  
579 alpha(2A)-adrenergic receptor. *Science* **377**, eabn7065, doi:10.1126/science.abn7065  
580 (2022).
- 581 7 Singh, I. *et al.* Structure-based discovery of conformationally selective inhibitors of the  
582 serotonin transporter. *Cell* **186**, 2160-2175 e2117, doi:10.1016/j.cell.2023.04.010 (2023).
- 583 8 Gahbauer, S. *et al.* Docking for EP4R antagonists active against inflammatory pain. *Nat*  
584 *Commun* **14**, 8067, doi:10.1038/s41467-023-43506-6 (2023).
- 585 9 Sadybekov, A. V. & Katritch, V. Computational approaches streamlining drug discovery.  
586 *Nature* **616**, 673-685, doi:10.1038/s41586-023-05905-z (2023).
- 587 10 Gorgulla, C. *et al.* A multi-pronged approach targeting SARS-CoV-2 proteins using ultra-  
588 large virtual screening. *iScience* **24**, 102021, doi:10.1016/j.isci.2020.102021 (2021).
- 589 11 Klarich, K., Goldman, B., Kramer, T., Riley, P. & Walters, W. P. Thompson Sampling  
590 horizontal line An Efficient Method for Searching Ultralarge Synthesis on Demand  
591 Databases. *J Chem Inf Model* **64**, 1158-1171, doi:10.1021/acs.jcim.3c01790 (2024).
- 592 12 Walters, W. P. Virtual Chemical Libraries. *J Med Chem* **62**, 1116-1124,  
593 doi:10.1021/acs.jmedchem.8b01048 (2019).
- 594 13 Gorgulla, C., Jayaraj, A., Fackeldey, K. & Arthanari, H. Emerging frontiers in virtual drug  
595 discovery: From quantum mechanical methods to deep learning approaches. *Curr Opin*  
596 *Chem Biol* **69**, 102156, doi:10.1016/j.cbpa.2022.102156 (2022).
- 597 14 Lyu, J., Irwin, J. J. & Shoichet, B. K. Modeling the expansion of virtual screening libraries.  
598 *Nat Chem Biol* **19**, 712-718, doi:10.1038/s41589-022-01234-w (2023).
- 599 15 Weston, G. S., Blazquez, J., Baquero, F. & Shoichet, B. K. Structure-based enhancement  
600 of boronic acid-based inhibitors of AmpC beta-lactamase. *J Med Chem* **41**, 4577-4586,  
601 doi:10.1021/jm980343w (1998).
- 602 16 Powers, R. A., Morandi, F. & Shoichet, B. K. Structure-based discovery of a novel,  
603 noncovalent inhibitor of AmpC beta-lactamase. *Structure* **10**, 1013-1023,  
604 doi:10.1016/s0969-2126(02)00799-2 (2002).
- 605 17 Feng, B. Y., Shelat, A., Doman, T. N., Guy, R. K. & Shoichet, B. K. High-throughput assays  
606 for promiscuous inhibitors. *Nat Chem Biol* **1**, 146-148, doi:10.1038/nchembio718 (2005).
- 607 18 Feng, B. Y. *et al.* A high-throughput screen for aggregation-based inhibition in a large  
608 compound library. *J Med Chem* **50**, 2385-2390, doi:10.1021/jm061317y (2007).
- 609 19 Eidam, O. *et al.* Design, synthesis, crystal structures, and antimicrobial activity of  
610 sulfonamide boronic acids as beta-lactamase inhibitors. *J Med Chem* **53**, 7852-7863,  
611 doi:10.1021/jm101015z (2010).
- 612 20 Babaoglu, K. *et al.* Comprehensive mechanistic analysis of hits from high-throughput and  
613 docking screens against beta-lactamase. *J Med Chem* **51**, 2502-2511,  
614 doi:10.1021/jm701500e (2008).

- 615 21 Gorgulla, C. *et al.* VirtualFlow 2.0 - The Next Generation Drug Discovery Platform Enabling  
616 Adaptive Screens of 69 Billion Molecules. *bioRxiv*, 2023.2004.2025.537981,  
617 doi:10.1101/2023.04.25.537981 (2023).
- 618 22 Bender, B. J. *et al.* A practical guide to large-scale docking. *Nat Protoc* **16**, 4799-4832,  
619 doi:10.1038/s41596-021-00597-z (2021).
- 620 23 Fassio, A. V. *et al.* Prioritizing Virtual Screening with Interpretable Interaction Fingerprints.  
621 *J Chem Inf Model* **62**, 4300-4318, doi:10.1021/acs.jcim.2c00695 (2022).
- 622 24 Cheng, Y. & Prusoff, W. H. Relationship between the inhibition constant (K<sub>1</sub>) and the  
623 concentration of inhibitor which causes 50 per cent inhibition (I<sub>50</sub>) of an enzymatic reaction.  
624 *Biochem Pharmacol* **22**, 3099-3108, doi:10.1016/0006-2952(73)90196-2 (1973).
- 625 25 McGovern, S. L., Helfand, B. T., Feng, B. & Shoichet, B. K. A specific mechanism of  
626 nonspecific inhibition. *J Med Chem* **46**, 4265-4272, doi:10.1021/jm030266r (2003).
- 627 26 Feng, B. Y. & Shoichet, B. K. A detergent-based assay for the detection of promiscuous  
628 inhibitors. *Nat Protoc* **1**, 550-553, doi:10.1038/nprot.2006.77 (2006).
- 629 27 O'Donnell, H. R., Tummino, T. A., Bardine, C., Craik, C. S. & Shoichet, B. K. Colloidal  
630 Aggregators in Biochemical SARS-CoV-2 Repurposing Screens. *J Med Chem* **64**, 17530-  
631 17539, doi:10.1021/acs.jmedchem.1c01547 (2021).
- 632 28 Walters, W. P. & Namchuk, M. Designing screens: how to make your hits a hit. *Nat Rev*  
633 *Drug Discov* **2**, 259-266, doi:10.1038/nrd1063 (2003).
- 634 29 Tirado-Rives, J. & Jorgensen, W. L. Contribution of conformer focusing to the uncertainty  
635 in predicting free energies for protein-ligand binding. *J Med Chem* **49**, 5880-5884,  
636 doi:10.1021/jm060763i (2006).
- 637 30 Irwin, J. J. & Shoichet, B. K. Docking Screens for Novel Ligands Conferring New Biology.  
638 *J Med Chem* **59**, 4103-4120, doi:10.1021/acs.jmedchem.5b02008 (2016).
- 639 31 Ackloo, S. *et al.* CACHE (Critical Assessment of Computational Hit-finding Experiments):  
640 A public-private partnership benchmarking initiative to enable the development of  
641 computational methods for hit-finding. *Nat Rev Chem* **6**, 287-295, doi:10.1038/s41570-  
642 022-00363-z (2022).
- 643 32 Gentile, F. *et al.* Artificial intelligence-enabled virtual screening of ultra-large chemical  
644 libraries with deep docking. *Nat Protoc* **17**, 672-697, doi:10.1038/s41596-021-00659-2  
645 (2022).
- 646 33 Yang, Y. *et al.* Efficient Exploration of Chemical Space with Docking and Deep Learning.  
647 *J Chem Theory Comput* **17**, 7106-7119, doi:10.1021/acs.jctc.1c00810 (2021).
- 648 34 Riley, B. T. *et al.* qFit 3: Protein and ligand multiconformer modeling for X-ray  
649 crystallographic and single-particle cryo-EM density maps. *Protein Sci* **30**, 270-285,  
650 doi:10.1002/pro.4001 (2021).
- 651 35 Fischer, M., Coleman, R. G., Fraser, J. S. & Shoichet, B. K. Incorporation of protein  
652 flexibility and conformational energy penalties in docking screens to improve ligand  
653 discovery. *Nat Chem* **6**, 575-583, doi:10.1038/nchem.1954 (2014).
- 654 36 Word, J. M., Lovell, S. C., Richardson, J. S. & Richardson, D. C. Asparagine and glutamine:  
655 using hydrogen atom contacts in the choice of side-chain amide orientation. *J Mol Biol*  
656 **285**, 1735-1747, doi:10.1006/jmbi.1998.2401 (1999).
- 657 37 Meng, E. C., Shoichet, B. K. & Kuntz, I. D. Automated Docking with Grid-Based Energy  
658 Evaluation. *J Comput Chem* **13**, 505-524, doi:DOI 10.1002/jcc.540130412 (1992).
- 659 38 Gallagher, K. & Sharp, K. Electrostatic contributions to heat capacity changes of DNA-  
660 ligand binding. *Biophys J* **75**, 769-776, doi:10.1016/S0006-3495(98)77566-6 (1998).
- 661 39 Sharp, K. A. Polyelectrolyte Electrostatics - Salt Dependence, Entropic, and Enthalpic  
662 Contributions to Free-Energy in the Nonlinear Poisson-Boltzmann Model. *Biopolymers* **36**,  
663 227-243, doi:DOI 10.1002/bip.360360210 (1995).
- 664 40 Mysinger, M. M. & Shoichet, B. K. Rapid context-dependent ligand desolvation in  
665 molecular docking. *J Chem Inf Model* **50**, 1561-1573, doi:10.1021/ci100214a (2010).

- 666 41 Coleman, R. G., Carchia, M., Sterling, T., Irwin, J. J. & Shoichet, B. K. Ligand pose and  
667 orientational sampling in molecular docking. *PLoS One* **8**, e75992,  
668 doi:10.1371/journal.pone.0075992 (2013).
- 669 42 Stein, R. M. *et al.* Property-Unmatched Decoys in Docking Benchmarks. *J Chem Inf Model*  
670 **61**, 699-714, doi:10.1021/acs.jcim.0c00598 (2021).
- 671 43 Tingle, B. I. *et al.* ZINC-22 horizontal line A Free Multi-Billion-Scale Database of Tangible  
672 Compounds for Ligand Discovery. *J Chem Inf Model* **63**, 1166-1176,  
673 doi:10.1021/acs.jcim.2c01253 (2023).
- 674 44 Eidam, O. *et al.* Fragment-guided design of subnanomolar beta-lactamase inhibitors  
675 active in vivo. *Proc Natl Acad Sci U S A* **109**, 17448-17453, doi:10.1073/pnas.1208337109  
676 (2012).
- 677 45 Liebschner, D. *et al.* Macromolecular structure determination using X-rays, neutrons and  
678 electrons: recent developments in Phenix. *Acta Crystallogr D Struct Biol* **75**, 861-877,  
679 doi:10.1107/S2059798319011471 (2019).
- 680 46 Emsley, P., Lohkamp, B., Scott, W. G. & Cowtan, K. Features and development of Coot.  
681 *Acta Crystallogr D Biol Crystallogr* **66**, 486-501, doi:10.1107/S0907444910007493 (2010).
- 682 47 Chen, V. B. *et al.* MolProbity: all-atom structure validation for macromolecular  
683 crystallography. *Acta Crystallogr D Biol Crystallogr* **66**, 12-21,  
684 doi:10.1107/S0907444909042073 (2010).
- 685 48 Pettersen, E. F. *et al.* UCSF ChimeraX: Structure visualization for researchers, educators,  
686 and developers. *Protein Sci* **30**, 70-82, doi:10.1002/pro.3943 (2021).

687